



Intelligent Virtual B-Scan Mirror (IVBM)

Michael Sommersperger¹(✉), Shervin Dehghani¹, Philipp Matten², Kristina Mach¹, Hessam Roodaki³, Ulrich Eck¹, and Nassir Navab¹

¹ Technical University of Munich, Munich, Germany

michael.sommersperger@tum.de

² Medical University of Vienna, Vienna, Austria

³ Carl Zeiss Meditec AG, Munich, Germany

Abstract. Swept-Source Optical Coherence Tomography (SS-OCT) allows surgeons to perform certain ophthalmic procedures under the exclusive guidance of real-time volumetric optical coherence tomography (4D OCT). In such scenarios, surgeons are no longer limited to rigid views through an operating microscope. Instead, direct volume rendering (DVR) of 4D OCT enables surgical maneuvers to be performed from arbitrary viewpoints. While 4D OCT maximizes the use of the depth-resolved OCT data by displaying it from an oblique perspective, performing complex instrument maneuvers from such views places a higher mental demand on the surgeon. In this work, we propose an Intelligent Virtual B-scan Mirror (IVBM), a novel concept for surgical 4D OCT visualization to provide additional guidance for targeted instrument interactions. The IVBM integrates a virtual mirror into a selected cross-section of the OCT volume. This mirror acts intelligently by only being sensitive to voxels associated with surgical instruments. Furthermore, volume structures aligned with the IVBM are highlighted, while structures behind the IVBM are preserved through an adaptive opacity transfer function. Unlike previous perceptual OCT visualization concepts, which primarily address depth perception in axial OCT direction, this novel approach aids surgical interactions from arbitrary views. This paper presents the definition and implementation of an IVBM in a 4D OCT integrated microscope. Our user study in a virtual simulation environment confirms the benefits and provides insights into the interaction with the concept.

Keywords: Optical Coherence Tomography · Surgical Visualization · Volume Raymarching · Virtual Mirrors

1 Introduction

Vitreoretinal surgeries are complex procedures that require extreme manual dexterity. Typically, surgeons operate through a stereoscopic microscope viewing the surgical area exclusively from an overhead perspective while manipulating delicate anatomical structures with sub-millimeter precision. In an effort to achieve

Supplementary Information The online version contains supplementary material available at https://doi.org/10.1007/978-3-031-43996-4_40.

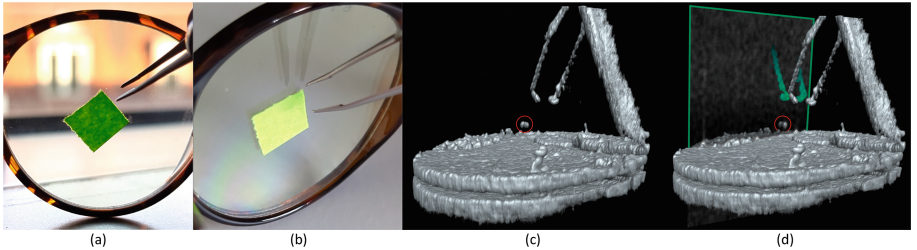


Fig. 1. (a) In daily life, navigating an instrument to a target is challenging without visual cues for distance perception. (b) Mirrors can provide additional views for improved targeting, see the reflection of the tweezers in the glass. (c) In 4D OCT-guided retinal surgery, navigating to a target is challenging from oblique views. (d) Our IVBM (outlined in green) leverages visual cues inspired by the reflective but transparent behavior illustrated in (b) for 4D OCT visualizations. (Color figure online)

improved surgical visualization, Optical Coherence Tomography (OCT) has been integrated into surgical microscopes, providing high-resolution depth-resolved imaging. Advances in spiral scanning and swept-source OCT [4,5,12] even paved the way for real-time volumetric imaging, enabling 4D visualizations of anatomical structures and surgical instruments. With the validation of intraoperative OCT through clinical studies [7,8], the emergence of 4D OCT systems prompts the anticipation of more precise and efficient microsurgical treatments. A common task in vitreoretinal surgery is to grasp and peel an Epiretinal Membrane (ERM), a $60\ \mu m$ [24] thin layer that forms on top of the retina, while avoiding to damage the on average $250\ \mu m$ thick retina [11].

GPU-accelerated direct volume rendering (DVR) was shown to be an effective way of visualizing surgical maneuvers, enabling real-time rendering of 4D OCT data on stereo displays [20]. Instead of viewing the surgical site from the top, as with stereoscopic microscopes, the depth-resolved properties of 4D OCT can be directly and fully utilized when oblique or even more extreme lateral views are provided [6]. This could even lead to more precise tool-tissue interactions since visualization of the surgical area from alternative viewpoints enables improved distance perception. This can be leveraged for instance when approaching small structures located at or above the retina during ERM or Internal Limiting Membrane (ILM) peeling [7,9]. On the other hand, such setups also introduce new complexities since surgical interaction from a lateral perspective is not common in current ophthalmic procedures. In particular, hand-eye coordination is naturally challenged when navigating instruments to a target from an uncommon view, imposing a higher mental demand on surgeons. To exploit the full potential of the 4D depth-resolved imaging modality, advanced visualization techniques could provide additional guidance and support complex maneuvers.

For this reason, we propose an *Intelligent Virtual B-scan Mirror (IVBM)*, a novel visualization concept to improve targeted instrument interactions in 4D OCT-guided surgery. As illustrated in Fig. 1, the concept of an IVBM is inspired

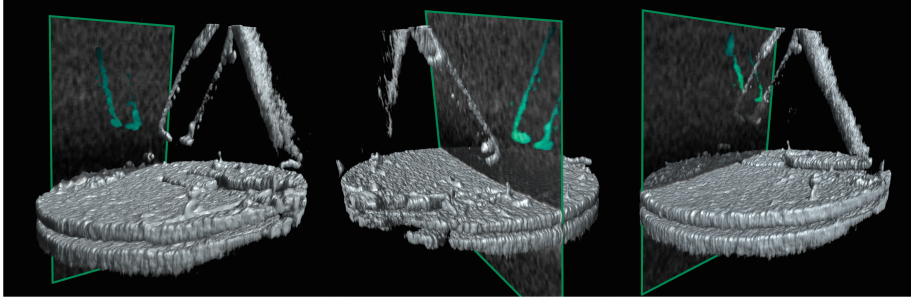


Fig. 2. The advantages of an *IVBM* include: (i) only voxels associated with surgical instruments are mirrored, while a perceptually linear color scheme is applied, which encodes the mirror distance (left), (ii) occluded instrument parts are visualized in the mirror view (middle) and (iii) the mirror is semi-transparent and integrated into a volume cross-section, visualizing tool and tissue structures behind it (right). The examples presented in this Figure show the IVBM outlined in green for better illustration.

by the reflective but at the same time transparent nature of glass. Conceptually, grasping an arbitrarily positioned object in space is challenging in the absence of depth cues. However, the reflections can provide an additional view that aids navigation to the target. Semi-transparency, on the other hand, preserves the background. We transfer this concept to volume raymarching in 4D OCT and integrate a mirror into a selected volume cross-section, which represents a virtual B-scan. While the IVBM highlights volume intensities within this virtual B-scan, it integrates an intelligent mirror, which is only sensitive to voxels that are close to the IVBM and associated with a surgical instrument. Volume structures behind the IVBM are preserved through an adaptive opacity transfer function. In addition, we leverage a perceptually linear color map to encode distance information and enhance the mirrored instrument in the IVBM. Compared to previous works, the proposed method particularly focuses on targeted instrument interactions from alternative viewpoints. The results of our user study provide detailed insights into user perception and interaction with the IVBM and emphasize the benefits for targeted maneuvers in 4D OCT-guided vitreoretinal surgery.

2 Related Work

Virtual mirrors have been initially proposed to support spatial perception and provide secondary views of virtual objects in augmented reality [1, 13, 19]. Applications have been introduced in angiography or laparoscopic surgery [15, 21] and effectiveness of a mirror view in medical scenarios has been shown in user studies with clinical experts [2]. Previous works on OCT volume visualization have so far solely focused on depth perception in axial OCT direction. These include applying a color transfer function based on the distance to a central reference depth [3] or to an identified retinal reference layer [22]. Other ways of providing

spatial cues include the augmentation of 2D OCT B-scans [17] or sound feedback to convey distance information [14].

As opposed to previous works on perceptual OCT visualization, the IVBM provides depth cues that aid targeted instrument navigation when viewing the surgical scene from a lateral perspective and targeting a specific cross-section, where axial depth perception is not a primary issue. Augmentation methods proposed in previous works are not designed for such scenarios. Previous works on virtual mirrors have mainly been implemented by rendering the scene from an alternative viewpoint and showing the mirror view next to the virtual objects. In contrast, we augment a selective mirror in-situ into a OCT cross-section.

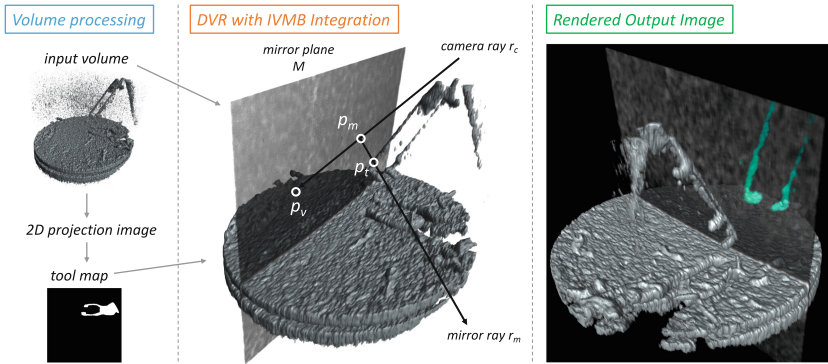


Fig. 3. Method overview: an OCT volume and a 2D instrument segmentation map are provided to the DVR algorithm. During volume raymarching, voxel intensities at the IVBM plane are highlighted and rendered transparent while intersections of the mirror ray with the instrument are integrated using a perceptually linear color map.

3 Methodology

3.1 Definition of an Intelligent Virtual B-Scan Mirror

We define an *Intelligent Virtual B-scan Mirror* (IVBM) as an augmentation of a selected virtual B-scan, which fulfills the following two requirements: (i) voxels integrated into the IVBM are highlighted in the volume rendering, while still visualized semi-transparent to preserve volume structures behind the IVBM. (ii) The selected B-scan cross-section acts as an intelligent mirror by only being sensitive to voxels associated with the surgical instruments in proximity to the IVBM. As illustrated in Fig. 2, the IVBM has the advantage of providing depth cues by visualizing the intersection of the instrument with the cross-section, when the instrument tip meets the tip of the mirrored instrument. It is also capable of visualizing instrument structures that are occluded in the direct view or located behind the IVBM cross-section and amplifies target structures that are

aligned with the IVBM. The following sections describe the required components, as well as the composition and direct integration of the IVBM in the volume raymarching algorithm.

3.2 Method Components

Since the IVBM integrates a mirror that is sensitive only to surgical instruments, mirror candidate voxels need to be identified in the volume. To achieve the real-time processing rates necessary for 4D OCT visualizations, we first identify the instrument in a 2D projection image of the volume. Inspired by [23], we create a 2D projection image that encodes the average intensity along each OCT A-scan. This image is forwarded to a Unet-like [16] convolutional neural network with ResNet34 [10] backbone to generate a binary instrument map M_{tool} . Since the OCT signal is fully blocked at the instrument surface, the anatomical structures below the instrument are obscured, and the corresponding A-scans contain only instrument-related voxels. Thus, the 3D position of the voxels associated with the instrument can be obtained by the detected A-scans in M_{tool} , as further described in Sect. 3.3. Before forwarding the OCT volume and the instrument map M_{tool} to the DVR algorithm, we additionally process the volume by applying a 3D median filter to reduce the OCT-typical speckle noise. An overview of the method is illustrated in Fig. 3. With this set of components in place, the composition of the IVBM is fully realized within the DVR algorithm, as described in the following section.

3.3 Composition of an Intelligent Virtual B-Scan Mirror

During volume raymarching, if a camera ray \vec{r}_c intersects with the IVBM, as shown in Fig. 3, three components contribute to the resulting ray color: (i) any voxel p_m along \vec{r}_c that is integrated into the IVBM, (ii) any voxel p_v along \vec{r}_c behind the IVBM and (iii) the specific voxel p_t , at which the mirror ray \vec{r}_m intersects with the surgical instrument. We define the IVBM plane M_{IVBM} as any arbitrary, either manually or automatically selected plane and can thus be defined by the general equation:

$$xn_x + yn_y + zn_z + d = 0 \quad (1)$$

where $\vec{n} = (n_x, n_y, n_z)$ specifies the normal of the plane. We define a distance threshold d_{IVBM} specifying the thickness of the IVBM. During volume raymarching, a voxel p_m with position (p_x, p_y, p_z) is integrated in the IVBM, if the following condition is fulfilled:

$$\left| \frac{|n_x p_x + n_y p_y + n_z p_z + d|}{\sqrt{n_x^2 + n_y^2 + n_z^2}} \right| < d_{IVBM} \quad (2)$$

To visualize the mirror reflections of surgical instruments, a mirror ray \vec{r}_m is cast from each point p_m obtained by (2). The mirror ray direction is determined by:

$$\vec{r}_m = \vec{r}_c - 2 \cdot \text{dot}(\vec{r}_c, \vec{n}) \cdot \vec{n} \quad (3)$$

During sampling along \vec{r}_m , we leverage the binary map M_{tool} and an intensity threshold $t_{tool} = 0.25$ (empirically obtained to discard OCT speckle noise), and select the mirrored instrument voxel p_t if the following condition is fulfilled:

$$M_{tool}(p_t) == 1 \wedge I(p_t) > t_{tool} \quad (4)$$

To mirror the instrument only when close to the IVBM, we limit the number of sampled steps n_{steps} along \vec{r}_m . In case of intersection with an instrument as determined by (4), the raymarching is terminated and the instrument reflection is augmented in the IVBM plane at p_m with color component C_{p_t} . In particular, we encode the distance along \vec{r}_m between p_m at the IVBM and p_t at the instrument by employing a perceptually linear color map. We employ the $L^*a^*b^*$ color space similar to [22] with the following modifications:

$$C_{L^*a^*b^*}(I, \delta^*) = \gamma(I) \cdot (\delta^* \cdot C_0 + (1 - \delta^*) \cdot C_1) \quad (5)$$

where $\delta^* = (i_m \cdot 0.7) / n_{steps}$ is a distance predicate that considers the step index $i_m \in [0, n_{steps}]$ along \vec{r}_m when reaching the instrument at p_t . Further, $\gamma(I)$ is a scaling factor as introduced in [22]. Choosing $C_0 = (I(p_t), -1.5, 1)$ and $C_1 = (I(p_t), -1.0, -1.0)$ achieves a color interpolation between blue hue when the instrument is further from the mirror and green hue when close to the mirror. The RGB component of the instrument reflection is then obtained with:

$$C_{p_t} = [RGB(C_{L^*a^*b^*}(I(p_t), \delta^*(p)))] \quad (6)$$

where $RGB(C)$ is an $L^*a^*b^*$ to RGB color space conversion. We additionally decrease the opacity of the reflections with increasing distance of the instrument to the mirror using $\sigma(p_t) = 1.0 - (step_m / n_{steps})^2$.

The overall appearance of a voxel at p_m , integrating instrument reflections while enhancing the natural intensities in the IVBM plane is finally defined by:

$$C(p_m) = [\mu \cdot I(p_m) \cdot (1 - \sigma(p_t)) + C_{p_t} \cdot \sigma(p_t), \alpha(\mu I(p_m))] \quad (7)$$

In practice, μ is a dynamically modifiable parameter to amplify the volume intensities of the virtual B-scan and $\alpha(I)$ is a conventional piece-wise linear opacity function. During volume raymarching, we use alpha blending to integrate the IVBM with the remaining volume structures as determined by (2). In general, voxels p_v that are not in the IVBM can be rendered using any convention for direct volume rendering. During our experiments and for the visualizations in Fig. 2 and Fig. 3 we use classic Phong shading as previously employed for OCT volume rendering [20]. In our visualizations, it provides structural surface details while visually highlighting the IVBM in the final rendering.

4 Experimental Setup and User Study

System Integration and Time Profiling. To evaluate if IVBMs can be deployed for the live display of 4D OCT data, we implemented the proposed concept in a C++ visualization framework. The 2D projection image generation and IVBM-integrated volume raymarching were implemented using OpenGL 4.6 and tested on a Windows 10 system with Intel Core i7-8700K @3.7 GHz and NVidia RTX 3090Ti GPU. We train our instrument segmentation network on a custom data set consisting of 3356 2D projection images generated from OCT volumes with a resolution of $391 \times 391 \times 644$ voxels that contain a synthetic eye model and a surgical forceps and include random rotations and flipping for data augmentation. We use PyTorch 1.13 and TensorRT 8.4 for model training and optimization. The data was labeled by two biomedical engineers.

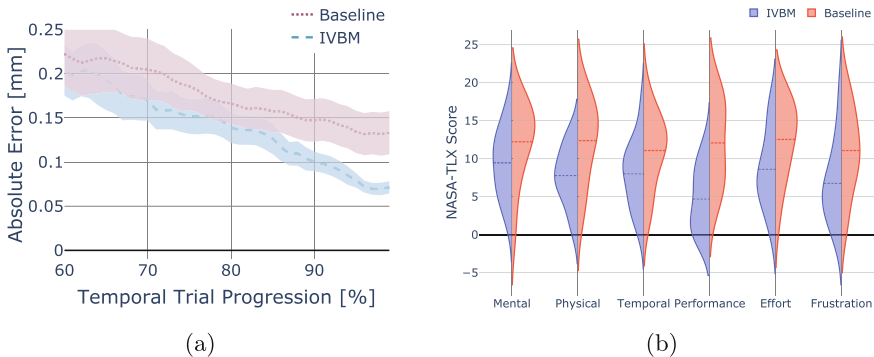


Fig. 4. Distance to the target over the course of the trial progression (a). Results of the subjective task load index based on NASA-TLX (b).

The average overall processing and rendering time, based on 20 test volumes with the same resolution, was 44.3 (± 3.1) ms (filter: 8.1 (± 1.2) ms, projection image generation and instrument segmentation: 5.7 (± 2.6) ms, rendering: 30.5 (± 0.6) ms). These benchmarks were achieved with $n_{steps} = 120$ mirror sample steps. To demonstrate the live 4D interactions, our method was integrated into the 4D SS-OCT system presented in [4], acquiring OCT volumes with resolution $391 \times 391 \times 644$ at 10 Hz volume update rates. In the supplementary materials, we include video recordings of instrument maneuvers in 4D OCT with our IVBM visualizations.

User Study. To determine if an IVBM could aid users in performing targeted instrument maneuvers under 4D OCT guidance, we conducted a user study in which we asked participants to move the tip of a surgical instrument to defined target locations. To achieve continuous, accurate, and efficient data collection during the study, we employ a virtual environment (Unity 2021.3) with simulated 4D OCT based on the method proposed in [18]. Additionally, a haptic 3D input device (3D Systems Geomagic Touch) was integrated to navigate

the virtual surgical instruments, where motion scaling of 4 : 1 was applied to reduce the influence of the individual manual tremor of the users. Small targets were generated on top of the retina, and the IVBM was automatically positioned at the target locations. To measure the effectiveness of the IVBM when interacting from uncommon perspectives, the virtual scene was rendered from a fixed view approximately orthogonal to the A-scan direction. As stereo vision through a microscope is an inherent part of common ophthalmic procedures, the simulation environment was displayed on an HTC Vive Pro headset leveraging stereo rendering. Users were asked to navigate the instrument tip to the target location and to press a button once satisfied with the positioning. The participants included in total 15 biomedical experts (12 male, 3 female) familiar with ophthalmology and OCT. The study was conducted in accordance with the declaration of Helsinki, the study data were anonymized, and vision tests were performed before the study to ensure healthy vision of all participants. After familiarizing themselves with the interaction in the virtual environment, participants performed 8 trials, with IVBM enabled. For ablation, the same number of trials were performed without IVBM, employing the method proposed in [20] for 4D OCT DVR with Phong shading as a baseline. The accuracy of the positioning and distance to the target was measured over the progression of the trials. Our results show that users reached the target with an average error of $70\text{ }\mu\text{m}$ ($\pm 40\text{ }\mu\text{m}$) when the IVBM was activated, while in baseline rendering an average error of $135\text{ }\mu\text{m}$ ($\pm 128\text{ }\mu\text{m}$) was measured, suggesting statistically significant differences between the distributions ($p < 0.002$ based on a Kruskal-Wallis test after detecting unequal variances). Furthermore, we analyzed the distance between the instrument tip and the target with respect to the progress of the trial. Figure 4a shows that when the IVBM was enabled, the deviation of the distance error continuously decreased, especially in the last quarter of the trial progressions, resulting in both more accurate and precise targeting. The outcomes of the NASA-TLX survey (Fig. 4b) conducted after the study showed improvements in all categories when the IVBM was activated. However, statistical significance could only be found in the categories performance ($p < 0.001$) and physical demand ($p < 0.02$) based on an ANOVA test for equal variances.

5 Discussion and Conclusion

Discussion. When users were provided an IVBM, statistically significant improvements regarding the targeting error were found. In a clinical setting, such as during retinal membrane peeling, similar improvements could make a substantial difference and may lead to a safer and more efficient treatment. The results of the subjective task load assessment were also overall improved when the IVBM was enabled, however, statistical significance could not be obtained in categories such as mental demand or frustration. Potential depth conflicts could be investigated in further studies and evaluated with clinical experts. Interestingly, a higher targeting accuracy was achieved with IVBM, even in cases when users reported a higher effort or judged their performance inferior compared to

baseline. An advantage of the IVBM is direct in-situ visualization that also highlights target structures, as users do not need to move their gaze from the surgical area to perceive the mirrored view. We envision an automatic identification of anatomical targets to find optimal IVBM positioning in the future.

Conclusion. We presented a novel visualization concept that augments a selected volume cross-section with an intelligent virtual mirror for targeted instrument navigation in 4D OCT. We have provided a definition and implementation of an IVBM and demonstrated its potential to effectively support surgical tasks and to be integrated into a 4D OCT system. We demonstrated the IVBM in simulated vitreoretinal surgery, however, we intend to further apply this concept also to other 4D medical imaging modalities.

Acknowledgements. This work is partially supported and the data is provided by Carl Zeiss Meditec. The authors wish to thank SynthesEyes (<https://syntheseyes.de>) for providing the excellent simulation setup for the user study.

References

1. Bichlmeier, C., Heining, S.M., Feuerstein, M., Navab, N.: The virtual mirror: a new interaction paradigm for augmented reality environments. *IEEE Trans. Med. Imaging* **28**(9), 1498–1510 (2009)
2. Bichlmeier, C., Heining, S.M., Rustaei, M., Navab, N.: Laparoscopic virtual mirror for understanding vessel structure evaluation study by twelve surgeons. In: 2007 6th IEEE and ACM International Symposium on Mixed and Augmented Reality, pp. 125–128. IEEE (2007)
3. Bleicher, I.D., Jackson-Atogi, M., Viehland, C., Gabr, H., Izatt, J.A., Toth, C.A.: Depth-based, motion-stabilized colorization of microscope-integrated optical coherence tomography volumes for microscope-independent microsurgery. *Transl. Vis. Sci. Technol.* **7**(6), 1–1 (2018)
4. Britten, A., et al.: Surgical microscope integrated MHz SS-OCT with live volumetric visualization. *Biomed. Optics Express* **14**(2), 846–865 (2023)
5. Carrasco-Zevallos, O.M., Viehland, C., Keller, B., McNabb, R.P., Kuo, A.N., Izatt, J.A.: Constant linear velocity spiral scanning for near video rate 4d oct ophthalmic and surgical imaging with isotropic transverse sampling. *Biomed. Optics Express* **9**(10), 5052 (2018)
6. Draefos, M., Keller, B., Toth, C., Kuo, A., Hauser, K., Izatt, J.: Teleoperating robots from arbitrary viewpoints in surgical contexts. In: 2017 IEEE/RSJ International Conference on Intelligent Robots and Systems (IROS), pp. 2549–2555 (2017)
7. Ehlers, J.P., et al.: Outcomes of intraoperative oct-assisted epiretinal membrane surgery from the pioneer study. *Ophthalmol. Retina* **2**(4), 263–267 (2018)

8. Ehlers, J.P., et al.: The DISCOVER study 3-year results: feasibility and usefulness of microscope-integrated intraoperative OCT during ophthalmic surgery. *Ophthalmology* **125**(7), 1014–1027 (2018)
9. Falkner-Radler, C.I., Glittenberg, C., Gabriel, M., Binder, S.: Intrasurgical microscope-integrated spectral domain optical coherence tomography-assisted membrane peeling. *Retina* **35**(10), 2100–2106 (2015)
10. He, K., Zhang, X., Ren, S., Sun, J.: Deep residual learning for image recognition. In: *Proceedings of the IEEE Conference on Computer Vision and Pattern Recognition*, pp. 770–778 (2016)
11. Jo, Y.J., Heo, D.W., Shin, Y.I., Kim, J.Y.: Diurnal variation of retina thickness measured with time domain and spectral domain optical coherence tomography in healthy subjects. *Invest. Ophthalmol. Vis. Sci.* **52**(9), 6497–6500 (2011)
12. Kolb, J.P., et al.: Live video rate volumetric OCT imaging of the retina with multi-MHz a-scan rates. *PLoS ONE* **14**(3), e0213144 (2019)
13. Li, N., Zhang, Z., Liu, C., Yang, Z., Fu, Y., Tian, F., Han, T., Fan, M.: vMirror: enhancing the interaction with occluded or distant objects in VR with virtual mirrors. In: *Proceedings of the 2021 CHI Conference on Human Factors in Computing Systems*, pp. 1–11 (2021)
14. Matinfar, S., et al.: Surgical Soundtracks: towards automatic musical augmentation of surgical procedures. In: Descoteaux, M., Maier-Hein, L., Franz, A., Jannin, P., Collins, D.L., Duchesne, S. (eds.) *MICCAI 2017. LNCS*, vol. 10434, pp. 673–681. Springer, Cham (2017). https://doi.org/10.1007/978-3-319-66185-8_76
15. Navab, N., Feuerstein, M., Bichlmeier, C.: Laparoscopic virtual mirror new interaction paradigm for monitor based augmented reality. In: *2007 IEEE Virtual Reality Conference*, pp. 43–50. IEEE (2007)
16. Ronneberger, O., Fischer, P., Brox, T.: U-Net: convolutional networks for biomedical image segmentation. In: Navab, N., Hornegger, J., Wells, W.M., Frangi, A.F. (eds.) *MICCAI 2015. LNCS*, vol. 9351, pp. 234–241. Springer, Cham (2015). https://doi.org/10.1007/978-3-319-24574-4_28
17. Roodaki, H., Filippatos, K., Eslami, A., Navab, N.: Introducing augmented reality to optical coherence tomography in ophthalmic microsurgery. In: *2015 IEEE International Symposium on Mixed and Augmented Reality*, pp. 1–6 (2015)
18. Sommersperger, M., et al.: Surgical scene generation and adversarial networks for physics-based iOCT synthesis. *Biomed. Optics Express* **13**(4), 2414–2430 (2022)
19. Tatzgern, M., Kalkofen, D., Grasset, R., Schmalstieg, D.: Embedded virtual views for augmented reality navigation. In: *Proceedings of the International Symposium Mixed Augmented Reality-Workshop Visualization in Mixed Reality Environments*, vol. 115, p. 123 (2011)
20. Viehland, C., et al.: Enhanced volumetric visualization for real time 4D intraoperative ophthalmic swept-source OCT. *Biomed. Optics Express* **7**(5), 1815–1829 (2016)
21. Wang, J., Fallavollita, P., Wang, L., Kreiser, M., Navab, N.: Augmented reality during angiography: integration of a virtual mirror for improved 2D/3D visualization. In: *2012 IEEE International Symposium on Mixed and Augmented Reality (ISMAR)*, pp. 257–264. IEEE (2012)
22. Weiss, J., Eck, U., Nasseri, M.A., Maier, M., Eslami, A., Navab, N.: Layer-aware iOCT volume rendering for retinal surgery. In: Kozlíková, B., Linsen, L., Vázquez, P.P., Lawonn, K., Raidou, R.G. (eds.) *Eurographics Workshop on Visual Computing for Biology and Medicine. The Eurographics Association* (2019)

23. Weiss, J., Sommersperger, M., Nasseri, A., Eslami, A., Eck, U., Navab, N.: Processing-aware real-time rendering for optimized tissue visualization in intraoperative 4D OCT. In: Martel, A.L., et al. (eds.) MICCAI 2020. LNCS, vol. 12265, pp. 267–276. Springer, Cham (2020). https://doi.org/10.1007/978-3-030-59722-1_26
24. Wilkins, J.R., et al.: Characterization of epiretinal membranes using optical coherence tomography. *Ophthalmology* **103**(12), 2142–2151 (1996)